

# Soft Matter

Accepted Manuscript



This is an *Accepted Manuscript*, which has been through the Royal Society of Chemistry peer review process and has been accepted for publication.

*Accepted Manuscripts* are published online shortly after acceptance, before technical editing, formatting and proof reading. Using this free service, authors can make their results available to the community, in citable form, before we publish the edited article. We will replace this *Accepted Manuscript* with the edited and formatted *Advance Article* as soon as it is available.

You can find more information about *Accepted Manuscripts* in the [Information for Authors](#).

Please note that technical editing may introduce minor changes to the text and/or graphics, which may alter content. The journal's standard [Terms & Conditions](#) and the [Ethical guidelines](#) still apply. In no event shall the Royal Society of Chemistry be held responsible for any errors or omissions in this *Accepted Manuscript* or any consequences arising from the use of any information it contains.

# **A molecular dynamics study of bond exchange reactions in covalent adaptable networks**

Hua Yang<sup>1,2</sup>, Kai Yu<sup>1</sup>, Xiaoming Mu<sup>1</sup>, Xinghua Shi<sup>3</sup>, Yujie Wei<sup>3</sup>, Yafang Guo<sup>2</sup>,  
H. Jerry Qi<sup>1\*</sup>

<sup>1</sup>The George W. Woodruff School of Mechanical Engineering, Georgia Institute of Technology, Atlanta, GA 30332, USA

<sup>2</sup>Department of Mechanics, School of Civil Engineering, Beijing JiaoTong University, Beijing, 100044, China

<sup>3</sup>State Key Laboratory of Nonlinear Mechanics, Institute of Mechanics, Chinese Academy of Sciences, Beijing, 100190, China

\* Corresponding author: [qih@me.gatech.edu](mailto:qih@me.gatech.edu)

**Abstract**

Covalent adaptable networks are polymers that can alter the arrangement of network connections by bond exchange reactions where an active unit attaches to an existing bond then kicks off its pre-existing peer to form a new bond. When the polymer is stretched, bond exchange reactions lead to stress relaxation and plastic deformation, or the so-called reforming. In addition, two pieces of polymers can be rejoined together without introducing additional monomers or chemicals on the interface, enabling welding and reprocessing. Although covalent adaptable networks have been researched extensively in the past, knowledge about the macromolecular level network alternations is limited. In this study, molecular dynamics simulations are used to investigate the macromolecular details of bond exchange reactions in a recently reported epoxy system. An algorithm for bond exchange reactions is first developed and applied to study a crosslinking network formed by epoxy resin DGEBA with the crosslinking agent tricarballylic acid. The trace of the active units is tracked to show the migration of these units within the network. Network properties, such as the distance between two neighboring crosslink sites, the chain angle, and the initial modulus are examined after each iteration of the bond exchange reactions to provide detailed information about how material behaviors and macromolecular structure evolve. Stress relaxation simulations are also conducted. It is found that even though bond exchange reactions change the macroscopic shape of the network, microscopic network characteristic features, such as the distance between two neighboring crosslink sites and the chain angle, relax back to the unstretched isotropic state. Comparison with a recent scaling theory also shows good agreement.

**Keywords:** Bond exchange reaction; covalent adaptable network; dynamic covalent network; active polymers; molecular dynamics simulations.

## 1. Introduction

Thermosets are polymers that have a crosslinked network, which offer several desired properties, such as excellent mechanical strength, thermal stability and solvent/environmental resistance (Shaw and MacKnight, 2005). In many of these polymers, the network is formed through crosslinking macromolecular chains by covalent bonds. Thus, the polymer network formation is irreversible, i.e., the polymer cannot flow upon heating and thus cannot be reshaped or recycled. In recent years, with the development of reversible networks, however, this conventional view starts to change. For example, the so-called covalent adaptable networks (CANs) (Bowman and Kloxin, 2012; Kloxin et al., 2010; Long et al., 2013b; Wojtecki et al., 2011), or dynamic covalent network (Rowan et al., 2002), combine the desirable attributes of conventional thermosets with the dynamic network structures. A typical CAN alternates its network through an addition-fragmentation process, as illustrated in Figure 1. An active unit attaches to an existing bond first (Fig. 1a); the newly formed tertiary structure is not stable, leading to one of the units being kicked-off, resulting in a new bond and an active unit (Fig. 1b, c). Such a reaction is often called a bond exchange reaction (BER). At the network level, BERs allow the network to be rearranged (Bergman and Wudl, 2008; Murphy et al., 2008), which leads to many interesting behaviors (Adzima et al., 2010; Park et al., 2010). For example, Scott et al (2005) demonstrated that light could trigger radical induced BERs for stress relaxation and plastic deformation. This material was later explored for a variety of applications, such as flaw retardation, surface patterning, foldable structures (Kloxin et al., 2011; Long et al., 2010; Long et al., 2011; Mu et al., 2015; Ryu et al., 2012). In Scott et al. (2005), radicals, which are produced from photolysis of photoinitiators, are required to maintain the BERs. Once photoinitiators are depleted, the BERs stop. Recently, Leibler's group proposed an epoxy-based CAN where the BERs are catalyzed and controlled by temperatures, which can be used for

thermoforming, welding, and powder-based reprocessing (Montarnal et al., 2011; Yu et al., 2014).

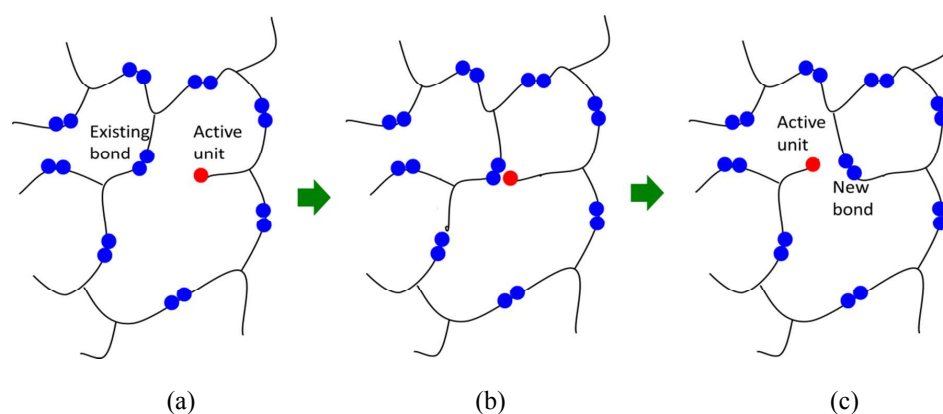


Figure 1. Schematic graphs of a bond exchange reaction: (a) before exchange; (b) intermediate state; (c) after exchange.

As a new group of active polymers, CANs have drawn significant interests in recent years, including new material systems developed by Lu et al (Lu et al., 2012) and Taynton et al (Taynton et al., 2014). Theoretical studies were conducted in the past. For example, Leibler and coworkers (1991) studied the diffusivity and stress relaxation in reversible network by considering the reptation of stickers, which are responsible for reversible crosslinks. Rubinstein and Semenov further studied the dynamics of thermoreversible gelation of associating polymer solutions (Rubinstein and Semenov, 1998, 2001; Semenov and Rubinstein, 1998). Recently, Long et al (Long et al., 2010; Long et al., 2009), Long et al (Long et al., 2013a, b), and Ma et al. (2014) studied the stress relaxation due to dynamic bonds in different material systems at continuum mechanics level. Stukhalin et al (2013) developed a scaling theory to study self-healing process by forming reversible bond with each other in hybrid reversible/permanent networks. Although these studies greatly advanced our understanding of these materials, it will be very helpful if we can delineate the macromolecular level details of network

rearrangement by BERs. For example, one fundamental question is if the BER-induced plastic deformation would change the structure of the network. Smallenburg et al (2013) used patchy particle model studied the swelling behaviors of reversible networks and found an entropy-driven phase separation. Molecular dynamics (MD) simulations (Frenkel and Smit, 2002) are a well-established and important tool that allows practical problems to be explored in details at macromolecular scales, which are difficult to extract directly from macroscopic experiments. For example, Yoshioka et al (Yoshioka et al., 2003) used MD simulations to examine glass transition temperature ( $T_g$ ) of the freeze-dried formulation containing polymer excipients. Li and Strachan (2011) performed an extensive characterization of the thermo-mechanical response of epoxy EPON862 with curing agent DETDA using MD simulations. Gou et al (2004) also conducted MD simulations to investigate the interface bonding of single-walled carbon nanotube reinforced epoxy composites. Bermejo and Ugarte studies the crosslinking process of PVA(Bermejo and Ugarte, 2009). For BERs, Rottach et al (2007) used coarse-grained approach to investigate stress relaxation of sequential crosslinking and scission of polymer networks, which focused mainly on stress relaxation. Bandyopadhyay(2011) proposed an MD method to simulate the sequence of bond formation and breakage with the goal of building an accurate network. In this work, we study the rearrangement of polymer network in the epoxy developed by Montarnal's work (Montarnal et al., 2011), where BERs are achieved through transesterification reactions. In that work, since the BERs are catalyzed and can continue as long as the temperature is high, it is reasonable not to consider the termination. The goal of this paper is to develop a full atomistic MD simulation procedure for BERs to study the evolution of polymer network. With the MD simulations, we can track the migration of active atoms during a relay of BERs. We also inspect several network properties, including the distance between two neighboring crosslink sites, the chain angles, initial modulus, stress relaxation, and shape reforming etc., for any changes in the network

during BERs. Finally, MD simulation of stress relaxation is compared with the existing theoretical works.

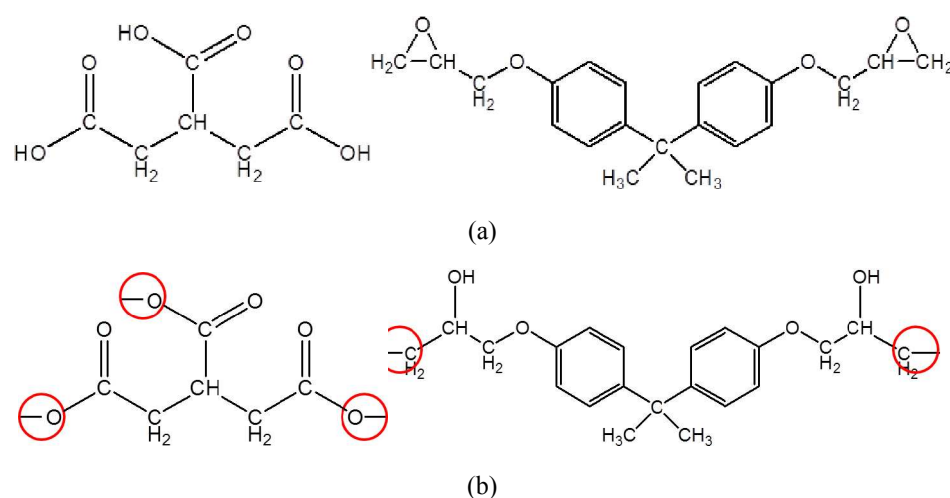


Figure 2. (a): Molecular structure of tricarballylic acid and DGEBA (b): Activation of tricarballylic acid and DGEBA ends for the crosslink. The atoms in the red circle showed their activity toward the crosslinking reaction.

## 2 Simulation Details

The MD model for the thermosetting epoxy network polymer with exchangeable bonds used in this study was prepared by following Montarnal's work (2010). The initial system consists of un-crosslinked epoxy resin DGEBA and crosslinking agent tricarballylic acid. The molecular structures are shown in Figure 2a, where a DGEBA has two active sites and a tricarballylic acid has three active sites. In order to maintain the 1:1 ratio among active sites in epoxy monomers and curing agent monomers, a mixture of 90 DGEBA molecules and 60 tricarballylic acid molecules, which results in a total atom number of 5430, was built using amorphous cell module in Materials Studio (Accelrys Software Inc., 2007) with charges assigned using the group charge method. All the simulations were performed using PCFF forcefield (Sun, 1995) and LAMMPS molecular dynamics software (Plimpton, 1995) as provided by Sandia National Laboratories. The Nose-Hoover thermostat and barostat (Hoover, 1985; Nose, 1984) were used for

temperature and pressure control, respectively. 3-D periodic boundary conditions were employed for all simulations to remove possible surface effects.

## 2.1 Crosslinking process

The first step in studying the BERs is to build a crosslinking network. The MD process of crosslinking epoxy resin compounds was investigated by many researchers and typically includes two parts: the first part is connection where monomers are connected by following a certain pre-defined criterion; the second part is relaxation where the artificial energy due to the connection part is relaxed. In addition, in order to avoid high artificial energy build-up in the connection part, an iterative approach is typically used to limit the number of connection reactions in one iteration. For example, in Xu and Wu's work (2006) only one connection reaction was allowed in each iteration, followed by 1000 time steps of MD relaxation of the newly formed topology. Apparently, this protocol requires a significant amount of computational time. Varshney et al (2008) combined Heine's dynamic crosslinking concept (Heine et al., 2004) by using a cutoff distance with Wu and Xu's iterative energy minimization method. Specifically, they connected all the atom pairs that meet the cutoff distance criterion. This would lead to a very dramatic system energy change if too many pairs were connected. Therefore, they used a multistep relaxation procedure for relaxing the system by gradually increasing the force constant. Varshney et al(2008) also compared three different crosslinking approaches where different active pairs may have preferred or equal chances of connection. Their results indicated that there was no significant difference among the final crosslinked systems, except the computational time.

In this work, we combine Wu and Xu's and Varshney's works, i.e., we use Varshney's method in the connection procedure and Wu and Xu's method in the relaxation procedure, which consists of one molecular mechanics (MM) energy minimization procedure followed by a MD relaxation. Figure 3 shows the flowchart of the method for crosslinking, which consists of 7 steps. In Step 1, the initial system is

equilibrated using NVT and NPT sequentially at the atmosphere pressure and 300 K for 100ps. Once the initial system is equilibrated, all the potential reactive sites in both tricarballic acid and DGEBA are activated. This is achieved by removing hydrogen atoms from tricarballic acid's carboxyl groups to make it chemically active. In the case of DGEBA, removing one of its hydrogen atoms creates a reactive methylene end group. It should be noted that although all the potential reactive sites are chemically activated in this step, two active sites are connected only when their relative distance is within a cutoff distance. In addition, following the observations from Varshney et al. (2008), we do not assign priorities to any reactive sites. The reactive macromolecular segments with reactive sites will be used in the next step. The schematics of reactive macromolecular segments are shown in Figure 2b.

After the initial preparation of the system in Step 1, Step 2 starts the iterative crosslinking process. In Step 2, a cutoff distance (4 Å) is defined. Step 3 conducts a NPT equilibrium for 100ps. The distances between all active atom pairs are checked in Step 4. If no pairs have the distance less than the cut-off distance, it is increased by 0.25Å and Step 3 is repeated. If at least one pair is found within the cut-off distance, the topological information is updated by introducing new bonds (formed by two atoms in these pairs), angles, dihedrals and proper angles into the system in Step 5, which is then followed by MM energy minimization and 100ps NPT relaxation in Step 6 to relieve any unfavorable interactions due to the formation of new bonds. Steps 3 to 6 are repeated until all the monomers are bonded together to form one network. Once the construction is completed, all non-hydrogen atoms in the system are saturated with hydrogen atoms in Step 7.

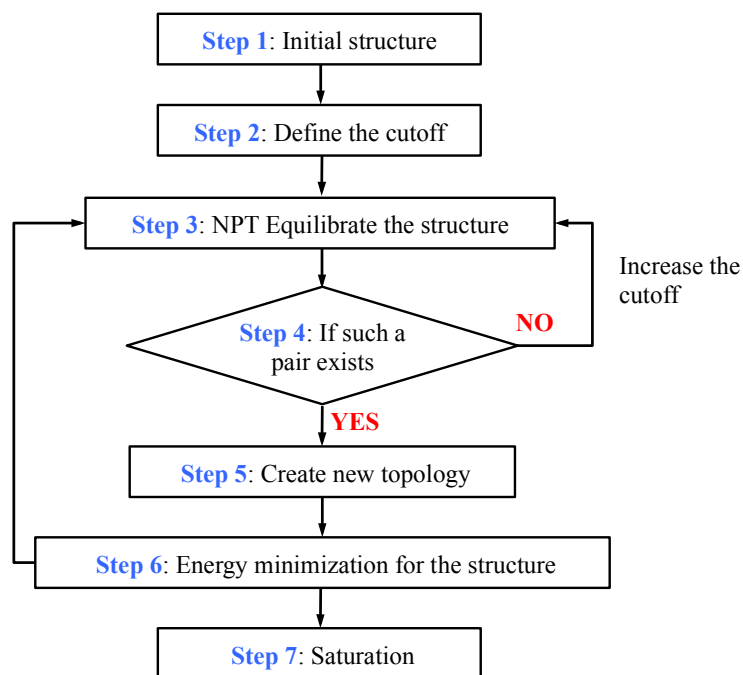


Figure 3. Flowchart of crosslink process

## 2.2 Bond exchange reaction process

Various kinds of reversible covalent chemistry can be used to produce CANs, such as Diels-Alder (DA) reaction (Chen et al., 2002), radical addition fragmentation chain transfer (RAFT) reaction (Moad et al., 2008) and transesterification reaction (Montarnal et al., 2011). In this work, the transesterification-type BER is used to enable the network rearrangement. The crosslinking process forms a network that contains ester and alcohol functional groups. The pendent alcohol and ester functional groups undergo a transesterification-type BER to enable the network rearrangement. The BER allowed in this system is illustrated in Figure 4, where a transesterification reaction occurs between an ester and an alcohol functional group (marked in red square in Figure 4a), resulting in a new ester functional group (red circle on the left in Figure 4b) and an alcohol functional group with a released oxygen (red circle on the right). The latter becomes active to continue the BER.

The flowchart describing the BER algorithm using MD method is shown in Figure 5. In Step 1, all the potential reactive sites in the network are activated by removing hydrogen atoms from the alcohol groups and by changing double bond into single bond in the ester functional groups. In the epoxy system in Montarnal, et al, (2011), BER is mediated by the presence of catalysts; we therefore assume that the catalysts are uniformly distributed. However, whether or not an active atom will be exchanged between two active sites depends on the relative distance, as well as the system energy after exchanging, which will be discussed in the followings.

The number of active oxygen atoms and active carbon atoms are both 180. These reactive molecular segments with reactive sites of oxygen or carbon will be used in the BERs. In addition, we assume that the BER only occurs between an alcohol and an ester functional group by following the reaction scheme shown in Figure 4. In Step 2, in order to avoid dramatic change in energy, a smaller initial cutoff distance (3.3 Å) is employed at the beginning of the simulation. The reactive system is then equilibrated in Step 3 by using the NVT ensemble for 100 ps at 450 K to achieve a relaxed network. In Step 4, the distances between all active pairs (one active hydrogen and one active oxygen) are calculated. In Step 5, any active pairs whose distances are within the cutoff distance are connected by forming new bonds. If no such a pair exists, Step 3 and step 4 will be repeated until such a pair can be found. In Step 6 and 7, the system energy is minimized then relaxed by using the NVT ensemble. In Step 8, the bond energies between the newly formed bond and the initial bond are compared. If the newly formed bond energy is lower than the initial bond energy, the initial bond is broken in Step 9 and vice versa. In Step 10, the topology information is updated by introducing new bonds, angles, dihedrals and improper angles into the system. Another round of minimization and 100 ps NVT relaxation were performed to relieve any unfavorable interactions due to the formation of new bonds. Steps 3 to 10 are repeated for 100 iterations.

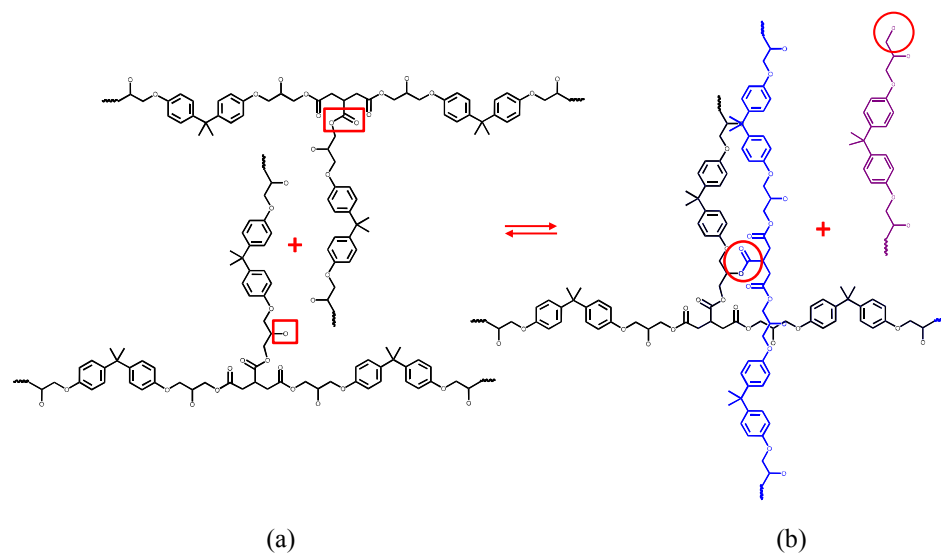


Figure 4. Schematic of bond exchange reaction (a) the transesterification reaction occurs between ester and alcohol functional groups, which are in the red square (b) after the transesterification, a new ester functional group (red circle on the left) is formed, and the released oxygen (red circle on the right) which belongs to alcohol functional group becomes an active atom again.

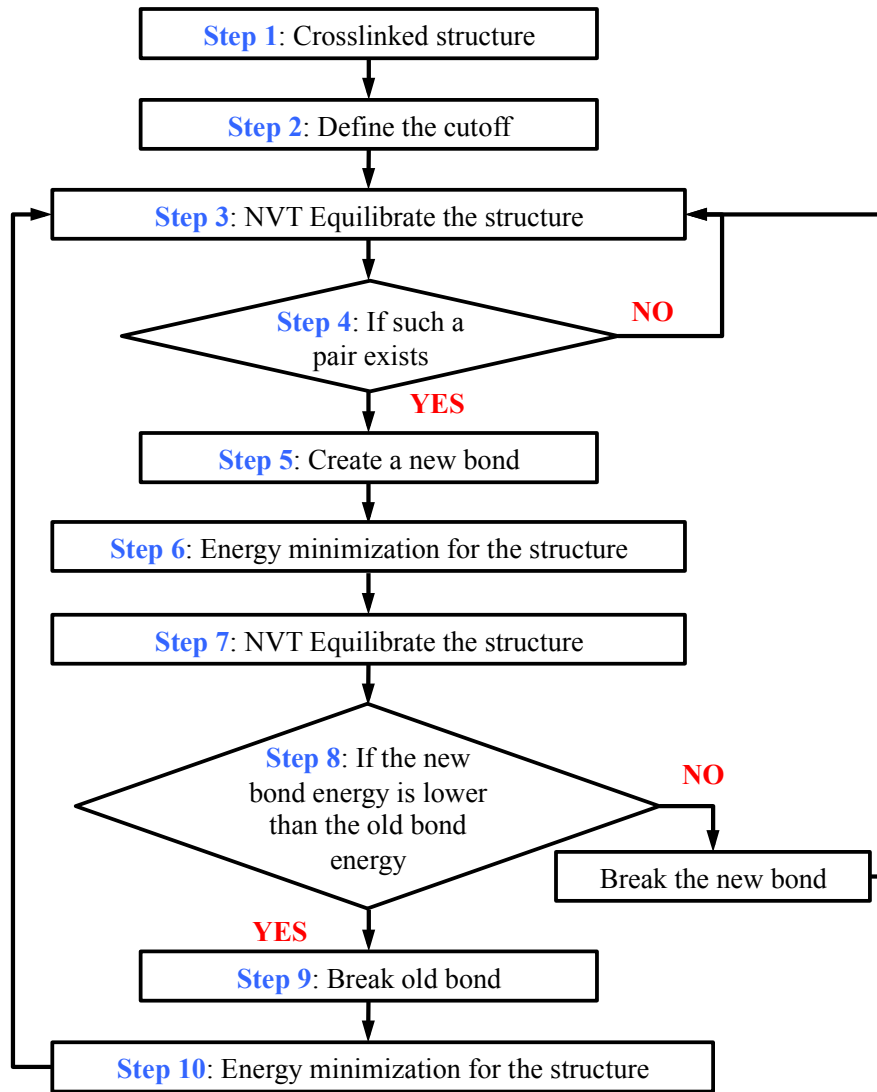


Figure 5. Flowchart of BER process

### 3 Results and discussions

#### 3.1 The Crosslinked System

The final crosslinked system is shown in Figure 6. The zoomed-in graph in Figure 6b confirms that the final network is an integrated structure. The glass transition temperature

is determined to be 312K for such a system (see Supplementary Materials for details).

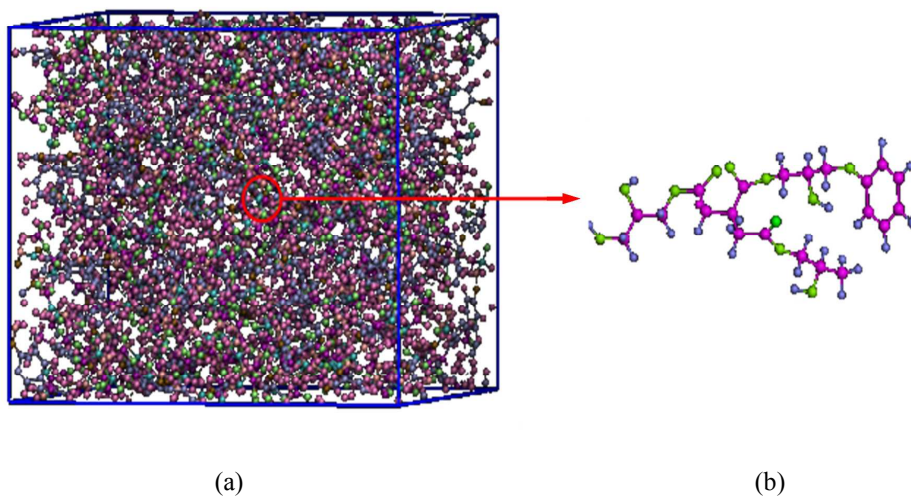


Figure 6. (a) The crosslinked network; (b) The zoomed-in view of the network. Carbon (pink); Oxygen (green); Hydrogen (purple)

### 3.2. Evolution of Network Properties

The BER process described above is used to conduct MD simulations. Here, in order to obtain a large enough sampling pool, we allow 100 iterations of BER process, which results in a total number of 605 BERs. Since there are 180 active oxygen atoms, all the active atoms participate in BER. The number of BERs in each iteration is shown in Figure S2 in Supplementary Materials. There is an average of  $\sim 6$  BERs in each iteration.

With the results from above simulations, we investigate the topological and mechanical properties during the evolution of network. We first track the trajectory of active atoms as they move around the macromolecular chains in the network. For topological properties, we monitor two important parameters: the distance between crosslinking sites and the chain angle. For mechanical properties, we check initial modulus as BERs proceed.

### 3.2.1 The trajectory of active atoms

In a BER, an active atom reacts with a functional group in the polymer chain, which subsequently generates a new bond and a new active atom that participates in the next BER. In such way, a BER continues in a relay of active atoms. It is therefore interesting to track the trajectory of active atoms in this relay, which is shown in Figure 7. The purple active atom (oxygen, purple color) at the end of a chain (cyan color) approaches a functional group (pink color in the green chain) in Figure 7a, then reacts with it by forming a new connected chain (cyan color and green color) and a new chain (green color) with an active atom at the end Figure 7b. The released active atom (oxygen, active) then continues to search for another functional group (blue pair) in Figure 7c and react with it in Figure 7d. Once the red atom forms a new bond with one blue atom (carbon), another blue atom (oxygen) is kicked off and becomes active again. This process continues. After 100 iterations of BER simulations, the relay goes through 11 BER reactions. The trajectory and its travel distance are shown in Figure 8a and Figure 8b. If more BER iterations are conducted, we expect that the trajectory of the relay would pervade the whole system, which is attributed to the fact that potential active atoms are randomly distributed within the system. Certainly, it would not be true if some termination mechanisms, such as bimolecular termination mechanism in radical assisted BERs, are considered. Figure 8c shows the average travel distance of all active atoms after 100 iterations of BERs, which are about 20 nanoseconds (ns) with ~600 BERs, showing clearly that with the BER process continues, the active atoms move further.

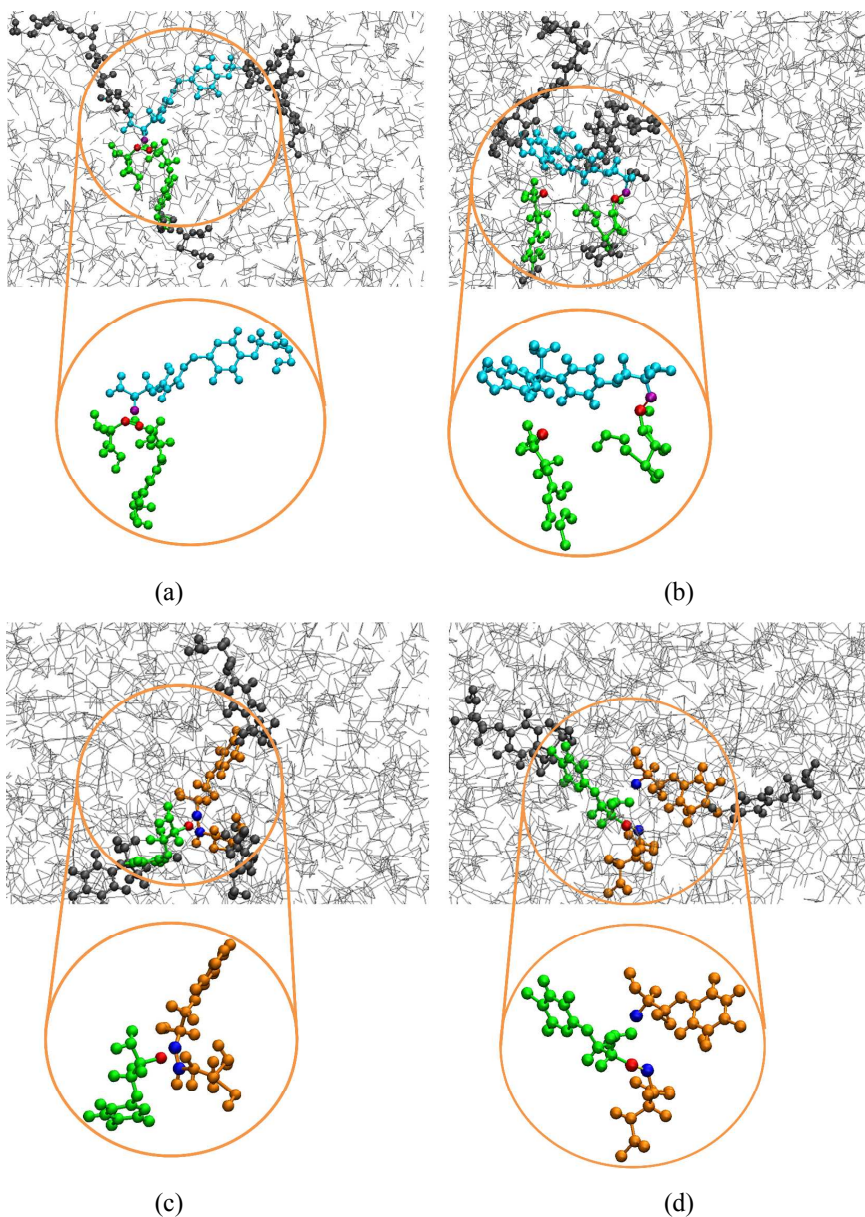
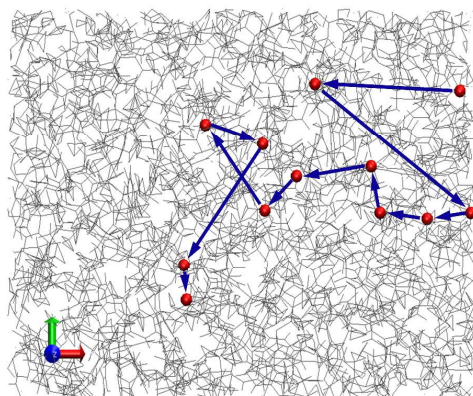
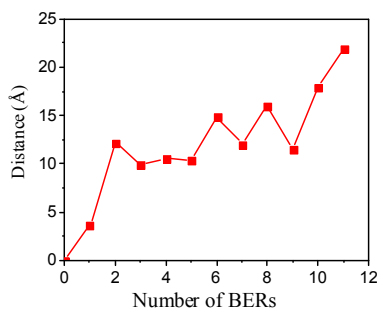


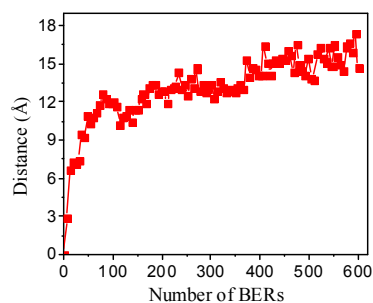
Figure 7. The relay of active atoms in BERs: (a) The purple active atom meets a red atom pair; (b) the purple atom reacts with the red atom pair by creating a new bond with one red atom and releasing the other red atom; (c) the released red atom meets a blue atom pair; (d) the red atom reacts with the blue pair by forming a new bond with one blue atom and releasing the other blue atom.



(a)



(b)



(c)

Figure 8. (a) The trajectory and (b) the travel distance of active atoms in 11 BERs in one relay. (c) The average travel distance of active atoms as a function of the number of BERs.

### 3.2.2 Evolution of network topological properties

To check the topological properties of the network, we use two parameters: the distance between crosslinking sites and the chain angle. The distance between two crosslinking sites is defined as the distance between two carbon atoms at the crosslink sites, as shown in Figure 9. The chain angle is the angle between the line connecting two crosslinking sites and one of the axes. Here, for the convenience, we use x-axis, which is the stretching direction in the next section.

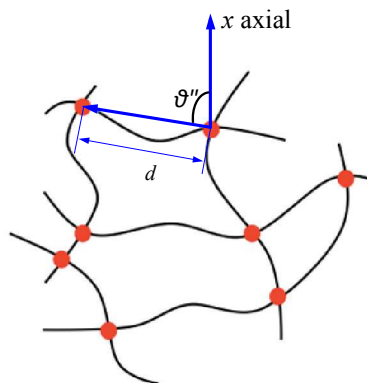


Figure 9. The schematic graph of the distance between two neighboring crosslink sites and the chain angle.

Figure 10 shows the average values and their standard deviations of the distance between two crosslinking sites and the chain angle. It can be seen that BERs do not change these network characteristics. The average distance between two neighboring crosslink sites remains to be  $15.6 \text{ \AA}$ , and the chain angle is  $58.8^\circ$ .

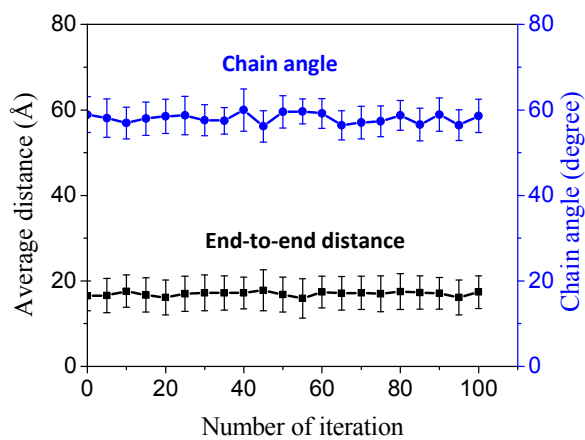


Figure 10. The average values and their standard deviations of the distance between two crosslinking sites and the chain angle.

The distributions of distance between two neighboring crosslink sites and the chain

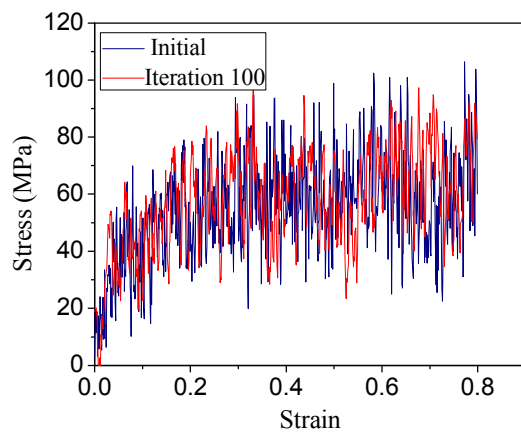
angle do not change during the BER process. Figure S3 (in Supplementary Materials) showed the distributions at the initial state, after 50 BER iterations and after 100 BER iterations. Student's t-Test method is used to compare if the network topology undergoes significant change. By comparing the distributions of the respective quantities between the initial system and the system in each BER iteration, we can obtain a two-tailed P value. If the P value is less than 0.05, the two samples are different from each other and on the other hand, the two samples are regarded to be the same. P values calculated in individual BER iterations are shown in Table 1. Since the P values are greater than 0.05, there are no significant changes in the distance between two neighbored crosslink sites and the chain angles.

Table 1. P value of distance between two neighboring crosslink sites and the chain angle in each iteration

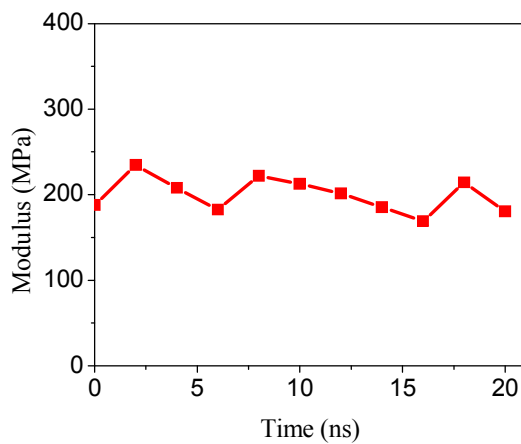
Iteration	10	20	30	40	50	60	70	80	90	100
Distance between two neighboring crosslink sites										
P value	0.287	0.488	0.147	0.76	0.679	0.314	0.208	0.078	0.267	0.347
Chain angle										
P value	0.203	0.429	0.172	0.298	0.307	0.532	0.183	0.304	0.129	0.097

### 3.2.3 Mechanical properties during BER

The MD simulations of uniaxial tensile tests are carried out on the initial system and the system after selected BER iterations at 450 K by continuously increasing the length of the simulation box along the x-direction and maintain the volume to be constant. Figure 11a presents the simulated stress-strain curves. In all the cases, the loading strain rate is  $1 \times 10^9 \text{ s}^{-1}$  and the maximum strain is 80%. The stress is determined by summing up the internal forces at individual particle points and dividing by the initial system area. The initial moduli are shown in Figure 11b. There is only a slight variation of the initial modulus, indicating that the BERs do not change the mechanical properties of the material.



(a)



(b)

Figure 11. (a) The stress-strain curves of the original system and the system after 100 BER iterations; (b) initial modulus as a function of time.

### 3.4 Stress relaxation and shape reforming

When the polymer is stretched, the network rearrangement due to BERs allows stress relaxation and shape reforming. In this section, the stress relaxation and reforming

behaviors are simulated. The end-to-end distance and the chain angle are calculated during the BER process to investigate how the BER induced stress relaxation influences the network. The crosslinked structure is stretched in the x-direction to 80% strain at the temperature of 450K with the loading rate of  $1 \times 10^9 \text{ s}^{-1}$ . The BER process is then performed using the method proposed above with NVT ensemble at 450K. After each BER iteration, the stress in the x-direction is obtained, which is shown in Figure 12a. It shows clearly that the stress relaxes as the BER process continues. Considering the time in each iteration is 200ps, we can estimate the stress relaxation time to be  $\sim 3500\text{ps}$  (see the dash line in Figure 12a). It should be also noted that although the stress can relax and the material behaves like a liquid when the BERs are on, the network always maintains its integrity. When the BERs are slowed (such as the temperature is low and the BER kinetics is becomes sluggish), the polymer behaves like a regular elastomer. If we turn off the BER, we see little stress relaxation (as shown in Figure S4 in Supplementary Materials).

The evolutions in the end-to-end distance and the chain angle during the tension process are shown in Figure 12b. With the deformation, the chain angle in the loading direction decreases to  $\sim 44^\circ$ , which is about a  $\sim 14^\circ$  drop, indicating that the chains are aligned in the stretching direction. The end-to-end distance increases by about  $\sim 2\text{\AA}$ . We compare the end-to-end vector in our simulation with theoretical prediction, which is a full network model of Wu and van de Giessen (Wu and Van Der Giessen, 1992, 1993). They assumed that chains are randomly distributed. Based on this assumption, the average chain orientation under a uniaxial stretching can be calculated as

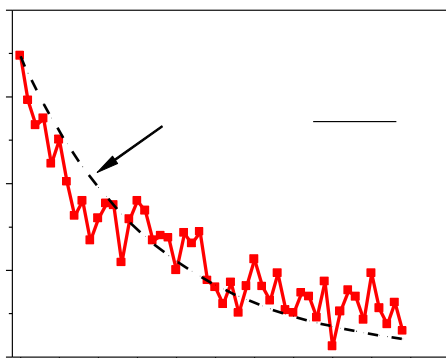
$$\bar{\theta} = \int_0^{\pi/2} \tan^{-1} \left( \frac{1}{\lambda_1^{3/2}} \tan \theta \right) \sin \theta d\theta, \quad (1)$$

where  $\lambda_1$  is the stretch and the elastomer is assumed to be incompressible. The average chain stretch can be calculated as

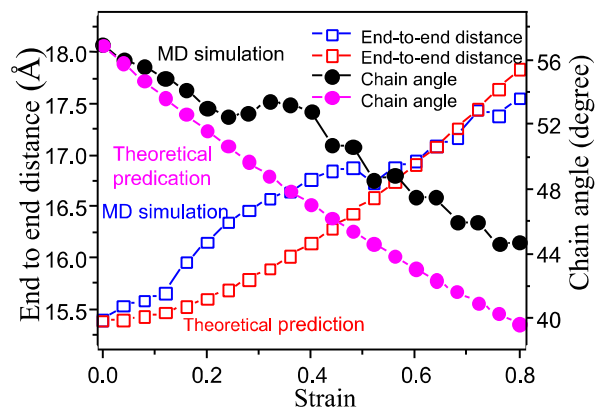
$$\bar{\lambda} = \int_0^{\pi/2} \sqrt{(\lambda_1 \cos \theta)^2 + \lambda_1^{-1} \sin^2 \theta} \sin \theta d\theta. \quad (2)$$

Figure 12(b) shows the comparison between the theoretical prediction and the MD simulation. It can be seen that MD simulation follows theoretical calculations.

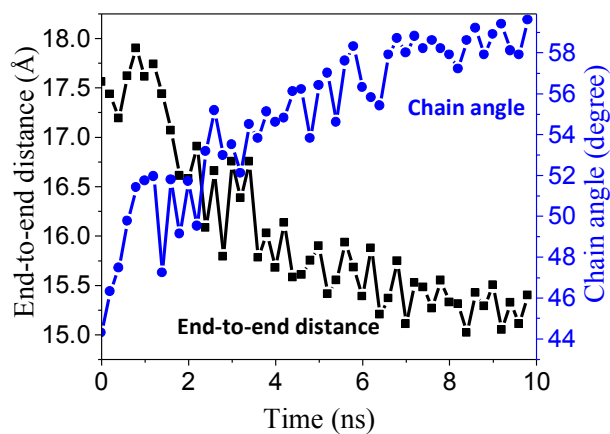
In the BER process, Figure 12c shows clearly that both the chain angle and the end-to-end distance recover to their original states, i.e., the chain angle increases to  $\sim 59^\circ$ , and the end-to-end distance decreases back to 15.5 Å. Both are close to their respective values in the unstretched isotropic state. These results indicate that although the tensile deformation changes the chain orientation, BER induced network rearrangement returns the network to its isotropic state.



(a)



(b)



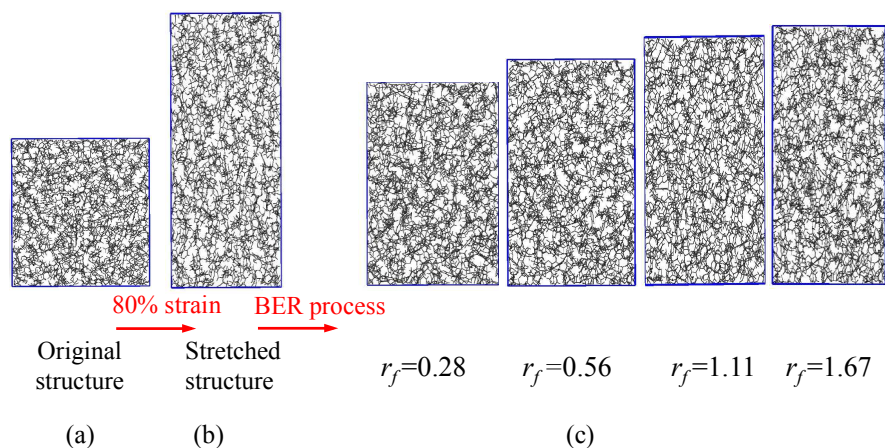
(c)

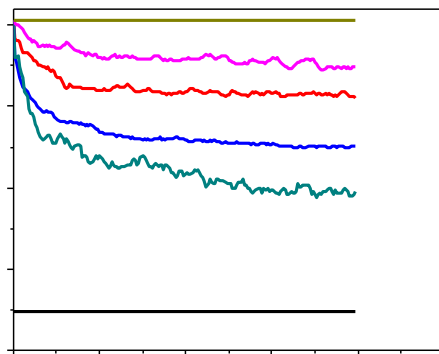
Figure 12. (a) Stress relaxation during the BER process; Evolutions of end to end distance and average chain angle (b) during the uniaxial tension, and (c) during BER iterations.

In order to observe how different numbers of BER events cause different levels of plastic deformation, the structure after each BER iteration is allowed to recover by removing the load and switching to a NPT relaxation for 500 ps at the temperature of 450

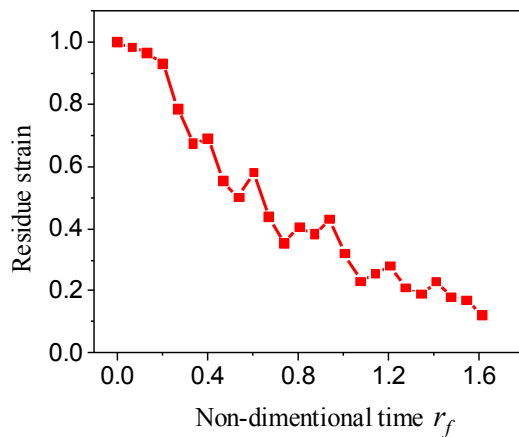
K and the atmospheric pressure. The box length in the stretched direction is measured to represent the shape change. Figure 13a shows the initial configuration of the simulation box and Figure 13b shows configuration after stretching. Figure 13c presents the unloaded boxes after different numbers of BERs (50 (at  $\sim 1.67ns$ ), 100 (at  $\sim 3.3ns$ ), 200 (at  $\sim 6.7ns$ ), and 300 (at  $\sim 10ns$ ), respectively). To provide a physical insight of this process, we define the rate of BER relaxation as the number of BERs per unit time and per active group. Using this definition and the fact that we are using 180 active groups and obtain 605 BERs in  $20ns$ , the BER rate is  $0.168ns^{-1}$ . Therefore, the BER relaxation time is  $\tau_{BER} = 5.95ns$ , which is close to the relaxation time measured from stress relaxation due to BERs (Fig. 12a,  $3.5ns$ ). We further normalize the times in Figure 13c by the BER relaxation time  $\tau_{BER}$  as  $r_f = t / \tau_{BER}$ . The shape of each box thus shows the residual strain (or shape fixity) after  $r_f$  amount of BER relaxation time. Figure 13d shows the recovery of the box during unloading at different  $r_f$ . The bottom and top lines represent the original and stretched lengths of the box, respectively. The residual strain is measured and shown in Figure 13e. The results clearly indicate that more BERs lead to better shape fixity.

Comment [MU1]: Response to comment 2.





(d)



(e)

Figure 13. BER induced plastic deformation and thermoforming. (a) The original structure. (b) The structure under 80% strain. (c) The structures after different number of BERs. (d) The box length of the structures with different number of BERs. (e) The residual strain during the BER process.

#### 4. Discussions

The MD simulations describe the network structure evolutions of covalent adaptable networks. It is interest to see if the simulated network properties are consistent with the predictions from existing theories, which will verify the effectiveness of the proposed simulation method. For network with reversible bonds, Gonzalez et al (1983, 1984) described the diffusion and the stress relaxation by a modified reptation model. However, his relaxation time had an exponential dependence on the average number of tie points per chain due to the assumption that the chain could only make a reptation step when it was simultaneously detached from all connections. Subsequently, Leibler and coworkers(Leibler et al., 1991) released such a restriction by assuming that an entangled polymer chain could move by breaking a few crosslinks, which showed a faster relaxation mechanism within the network. The developed sticky reptation theory demonstrated excellent capability in predicting the dynamics of reversible networks compared with the Gonzalez's theory, which typically exhibited several orders of magnitude deviation from the experimental data, especially when the material viscous behavior was obvious. Recently, Stukhalin and coworkers(Stukalin et al., 2013) developed a scaling theory to investigate self-healing process in reversible networks, which was modeled by a system consisting of dangling chains with reversible stickers at one end attached to a permanently crosslinked network at the other end. They also found that the bond lifetime was the relevant time scale for the description of the stress relaxation in reversible networks. In the following discussion, the self-diffusion coefficient of the epoxy network calculated from the relaxation time is compared with those in Leibler and coworkers' theory (Leibler et al., 1991) and Stukhalin and coworkers' theory(Stukalin et al., 2013). The relationship between the bonding time and the relaxation time in the MD simulation is also compared with Stukhalin and coworkers' theory.

In Leibler et al (1991), the self-diffusion coefficient is derived as :

$$D \cong \frac{a^2}{2\tau S^2} \left(1 - \frac{9}{p} + \frac{12}{p^2}\right), \quad (3)$$

where  $a$  ( $a \cong bN^{1/2}$ ) is the average end to end distance with  $b$  denoting the monomer length and  $N$  denoting the number of monomers between two crosslink sites,  $S$  is the number of stickers attached to each chain. For the epoxy network,  $a = 15.6 \text{ \AA}$ ,  $S = 5$ .  $\tau$  is the average lifetime of free stickers and  $p$  is the average fraction of stickers that are closed. According to Stukalin et al (2013),  $p$  can also be calculated as the fraction of lifetime of closed stickers, i.e.  $p = t_c / (t_c + t_o)$ , where  $t_c$  is the lifetime of the closed stickers and  $t_o$  is the lifetime of the free (open) ones. The average lifetimes of free stickers and closed stickers are shown in Table 2. The initial low lifetime is due to the relatively small sampling space at the beginning of the simulation.

Table 2. Average lifetime of closed stickers and free stickers during BER process, fraction of closed stickers during BER process

Iteration	10	20	30	40	50	60	70	80	90	100
Average lifetime of closed stickers (ps)	1312	2216	3128	3576	3072	3903	3798	3715	4094	3849
Average lifetime of free stickers (ps)	1633	2046	2103	1967	2284	2198	2376	2388	2217	2109
$p$	0.45	0.52	0.6	0.65	0.57	0.64	0.62	0.61	0.65	0.65

According to Leibler's et al (1991), the self-diffusion coefficient of reversible networks can be directly related to the stress relaxation time  $\tau_d$  as:

$$D = \frac{a^2}{\tau_d}. \quad (4)$$

This relaxation time of the epoxy system during the MD simulation is determined to be 3500ps from Figure 12 (a).

In Stukhalin et al (2013), the dynamics of open stickers in the partner exchange regime can be described as follows:

$$D = R_0^2 / \tau_b , \quad (5)$$

where  $R_0 \approx bN^{1/2}$ ,  $D$  is the effective diffusion coefficient for partner exchange,  $\tau_b$  is the average time two stickers spend in a bonded state before a successful separation on molecular distance.

It should be noted that in Eqs. 3-5, the average lifetime of free stickers  $\tau$  and the stress relaxation time  $\tau_d$  depend on the iteration times during the MD simulation. However, due to their linear relationship with the simulation time, the comparison of the computed self-diffusion coefficients in Eqs. 3-5 is independent of the timing scale that we choose for the simulation.

The diffusion coefficients obtained from Leibler's theoretical prediction (Eq. 3), stress relaxation time (Eq. 4) and Stukhalin's theoretical prediction (Eq.5) are plotted in Figure 14 as a function of time. The diffusivity from stress-relaxation simulation matches very closely with Stukhalin and co-workers' prediction. The first two points in theoretical prediction shows higher values, which could be due to the smaller sampling points for the lifetime of active atoms at the beginning of the simulation. These results confirm the effectiveness of Stukhalin and coworkers' theory in studying the dynamics of reversible covalent network.

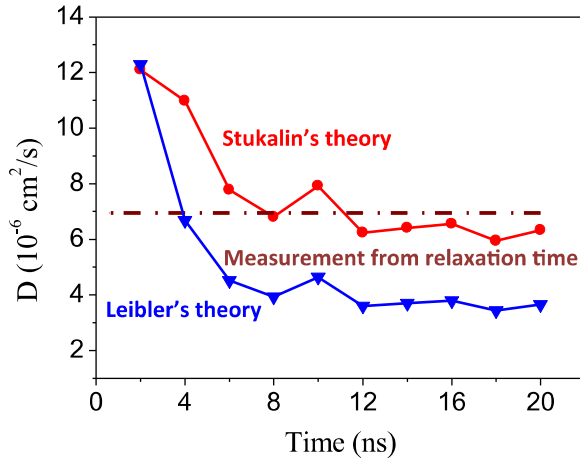


Figure 14. Diffusion coefficients from theoretical results and relaxation time

In Stukhalin and coworkers' work (2013), average lifetime of closed stickers is derived as:

$$\tau_b \approx \tau_0 \exp(\varepsilon / k_B T). \quad (6)$$

The average lifetime of closed stickers is equal to the time needed for a single BER (Stukalin et al., 2013). We assume that there are  $\xi$  dangling chains in a unit volume, which means there are  $\xi$  possible exchangeable bonds. During a time interval  $dt$ , a single exchangeable bond finishes  $\frac{dt}{\tau_b}$  BERs, the total number of BERs is  $\xi \frac{dt}{\tau_b}$ . We

also assume that after a single BER, the internal force in a single chain is totally released, the drop of stress can be related to the number of BER, which can be described as:

$$\frac{d\sigma}{\sigma} = \frac{\xi \frac{dt}{\tau_b}}{\xi} = \frac{dt}{\tau_b}. \quad (7)$$

Hence,

$$\sigma(t) = \sigma_0 \exp\left(-\frac{t}{\tau_b}\right). \quad (8)$$

Thus we have  $\tau = \tau_b$ , which means the relaxation time is equal to the lifetime of closed stickers.

The relaxation time and the average lifetime of closed stickers during BER process in our MD simulation is plotted in Figure 15. The first two points of the average lifetime of closed stickers curve show smaller value could be due to the small sample space. The simulation results indicate that the average lifetime of closed stickers is very close to the relaxation time of the system, which confirms the effectiveness of Stukhalin and coworkers' theory.

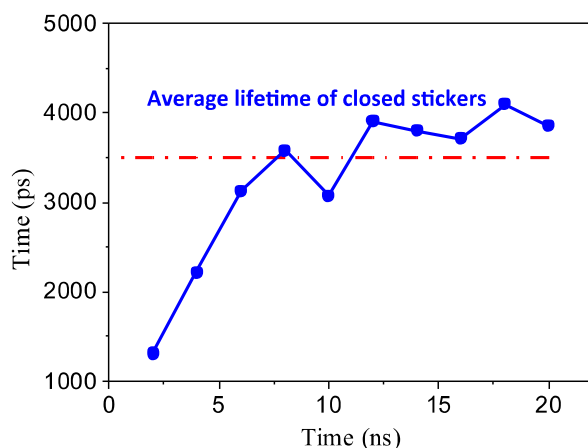


Figure 15. The average lifetime of closed stickers and the relaxation time during BER process

For a network polymer that can undergo the BER process, there are two relaxation mechanisms. The first one is the conventional relaxation mechanism that is due to chain diffusion and the second one is due to BERs. Since both relaxation mechanisms can relax stress, it is important to distinguish their contributions. Here, we can obtain the relaxation

time due to chain diffusion by using uniaxial tensile simulations and stress relaxation simulations where the BERs are turned off (see Supplementary Materials). From these simulations, we found that the relaxation time due to chain diffusion is  $\sim 2-6ps$ , which is much smaller than the relaxation time due to BERs ( $3.5-6ns$ ). Therefore, in the simulations studied in this paper, the BERs are the dominant relaxation mechanism. It should be noted that in the epoxy system by Montarnal et al (2011), BERs occur at temperatures significantly higher than  $T_g$ , where the relaxation due to chain diffusion becomes significantly efficient (so the relaxation time is very small). As the temperature is lowered, BER rates become slower but chain diffusions are less efficient; we should see a crossover the relaxation times. Eventually, at the temperature around  $T_g$ , BER rates become almost zero and the relaxation due to chain diffusion will dominate.

Comment [MU3]: Response to comment 2.

It should be noted that the 90 chain system in our simulations is relatively small and may have some structure differences as compared a larger system, especially infinitely large network system. Such a difference and its impact to the BERs should be studied in the future. The results from this paper should be limited to the small system.

Comment [MU4]: Response to comment 1.

## 5. Conclusions

In this work, a detailed full atomistic molecular dynamic simulation methodology for bond exchange reactions in covalent adaptable network is proposed. The simulations show clearly how an active group undergoes an exchange reaction, resulting in bond exchange and formation of a new active group, which subsequently undergoes additional exchange reactions. Based on the simulations, the distance between neighbored crosslink sites, the chain angle, and the material initial modulus during bond exchange reaction process are calculated. The results indicate that covalent adaptable network can maintain its network integrity and mechanical properties during bond exchange reactions. Besides, the stress relaxation and thermoforming behaviors are investigated. The results indicate that although the bond exchange reactions lead to the macroscopic phenomena of stress

relaxation, plastic deformation and thermoforming, the end-to-end distance and the chain angle return to their original isotropic states at the macromolecular level. In addition, the comparison with the theoretical work by Stukhalin et al (2013) confirms the effectiveness of their theory. Although the bond exchange reaction mechanism studied in this paper is limited to transesterification, this method can be extended to other covalent adaptable networks, such as Diels-Alder materials and RAFT network to investigate the macromolecular mechanisms. In addition, this method opens an avenue to further research for covalent adaptable networks, such as surface welding, which is currently undergoing and will be reported in the future.

#### Acknowledgement

HJQ, HY, KY and XM acknowledge the financial support from US National Science Foundation (CMMI-1404627). KY and XM also acknowledge the support from National Natural Science Foundation of China (11472207). HY acknowledges the financial support from Chinese Scholarship Council. XS acknowledges the support from NSFC (11023001). The authors also acknowledge the help and the discussions with the anonymous reviewer, whose insightful comments greatly improve the paper.

Comment [MU5]: Overall.

#### Reference

- Accelrys Software Inc., 2007. Discovery Studio Modeling Environment: Release 5.5, San Diego.
- Adzima, B.J., Kloxin, C.J., Bowman, C.N., 2010. Externally Triggered Healing of a Thermoreversible Covalent Network via Self-Limited Hysteresis Heating. *Advanced Materials* 22, 2784-+.
- Bandyopadhyay, A., Valavala, P.K., Clancy, T.C., Wise, K.E., Odegard, G.M., 2011. Molecular modeling of crosslinked epoxy polymers: The effect of crosslink density on thermomechanical properties. *Polymer* 52, 2445-2452.
- Bergman, S.D., Wudl, F., 2008. Mendable polymers. *Journal of Materials Chemistry* 18, 41-62.
- Bermejo, J.S., Ugarte, C.M., 2009. Chemical Crosslinking of PVA and Prediction of Material Properties by Means of Fully Atomistic MD Simulations. *Macromol Theor Simul* 18, 259-267.

- Bowman, C.N., Kloxin, C.J., 2012. Covalent Adaptable Networks: Reversible Bond Structures Incorporated in Polymer Networks. *Angewandte Chemie-International Edition* 51, 4272-4274.
- Chen, X.X., Dam, M.A., Ono, K., Mal, A., Shen, H.B., Nutt, S.R., Sheran, K., Wudl, F., 2002. A thermally re-mendable cross-linked polymeric material. *Science* 295, 1698-1702.
- Frenkel, D., Smit, B., 2002. *Understanding molecular simulation: from algorithms to applications*. Elsevier: New York.
- Gonzalez, A.E., 1983. Viscosity of Ionomer Gels. *Polymer* 24, 77-80.
- Gonzalez, A.E., 1984. Viscoelasticity of Ionomer Gels .2. The Elastic-Moduli. *Polymer* 25, 1469-1474.
- Gou, J.H., Minaie, B., Wang, B., Liang, Z.Y., Zhang, C., 2004. Computational and experimental study of interfacial bonding of single-walled nanotube reinforced composites. *Computational Materials Science* 31, 225-236.
- Heine, D.R., Grest, G.S., Lorenz, C.D., Tsige, M., Stevens, M.J., 2004. Atomistic simulations of end-linked poly(dimethylsiloxane) networks: Structure and relaxation. *Macromolecules* 37, 3857-3864.
- Hoover, W.G., 1985. CANONICAL DYNAMICS - EQUILIBRIUM PHASE-SPACE DISTRIBUTIONS. *Physical Review A* 31, 1695-1697.
- Kloxin, C.J., Scott, T.F., Adzima, B.J., Bowman, C.N., 2010. Covalent Adaptable Networks (CANS): A Unique Paradigm in Cross-Linked Polymers. *Macromolecules* 43, 2643-2653.
- Kloxin, C.J., Scott, T.F., Park, H.Y., Bowman, C.N., 2011. Mechanophotopatterning on a Photoresponsive Elastomer. *Advanced Materials* 23, 1977-1981.
- Leibler, L., Rubinstein, M., Colby, R.H., 1991. Dynamics of Reversible Networks. *Macromolecules* 24, 4701-4707.
- Li, C., Strachan, A., 2011. Molecular dynamics predictions of thermal and mechanical properties of thermoset polymer EPON862/DETDA. *Polymer* 52, 2920-2928.
- Long, K., Dunn, M., Qi, H., 2010. Mechanics of soft active materials with phase evolution. *Int J Plasticity* 26, 603-616.
- Long, K., Scott, T., Qi, H., Bowman, C., Dunn, M., 2009. Photomechanics of light-activated polymers. *Journal of Mechanics and Physics of Solids* 57, 1103-1121.
- Long, K.N., Scott, T.F., Dunn, M.L., Qi, H.J., 2011. Photo-induced deformation of active polymer films: Single spot irradiation. *International Journal of Solids and Structures* 48, 2089-2101.
- Long, R., Qi, H.J., Dunn, M.L., 2013a. Modeling the mechanics of covalently adaptable polymer networks with temperature-dependent bond exchange reactions. *Soft Matter* 9, 4083-4096.
- Long, R., Qi, H.J., Dunn, M.L., 2013b. Thermodynamics and mechanics of photochemically reacting polymers. *Journal of the Mechanics and Physics of Solids* 61, 2212-2239.
- Lu, Y.-X., Tournilhac, F., Leibler, L., Guan, Z., 2012. Making Insoluble Polymer

- Networks Malleable via Olefin Metathesis. *Journal of the American Chemical Society* 134, 8424-8427.
- Ma, J., Mu, X., Bowman, C.N., Sun, Y., Dunn, M.L., Qi, H.J., FANG, D., 2014. A Photoviscoplastic Model for Photo Activated Covalent Adaptive Networks. *Journal of Mechanics and Physics of Solids* 70, 84-103.
- Moad, G., Rizzardo, E., Thang, S.H., 2008. Radical addition-fragmentation chemistry in polymer synthesis. *Polymer* 49, 1079-1131.
- Montarnal, D., Capelot, M., Tournilhac, F., Leibler, L., 2011. Silica-Like Malleable Materials from Permanent Organic Networks. *Science* 334, 965-968.
- Montarnal, D., Tournilhac, F., Hidalgo, M., Leibler, L., 2010. Epoxy-Based Networks Combining Chemical and Supramolecular Hydrogen-Bonding Crosslinks. *J Polym Sci Pol Chem* 48, 1133-1141.
- Mu, X., Sowan, N., Tumbic, J.A., Bowman, C.N., Mather, P.T., Qi, H.J., 2015. Photo-Induced Bending in a Light-Activated Polymer Laminated Composite. *Soft Matter* 11, 2673-2682.
- Murphy, E.B., Bolanos, E., Schaffner-Hamann, C., Wudl, F., Nutt, S.R., Auad, M.L., 2008. Synthesis and characterization of a single-component thermally remendable polymer network: Staudinger and Stille revisited. *Macromolecules* 41, 5203-5209.
- Nose, S., 1984. A UNIFIED FORMULATION OF THE CONSTANT TEMPERATURE MOLECULAR-DYNAMICS METHODS. *Journal of Chemical Physics* 81, 511-519.
- Park, H.Y., Kloxin, C.J., Scott, T.F., Bowman, C.N., 2010. Covalent adaptable networks as dental restorative resins: Stress relaxation by additionfragmentation chain transfer in allyl sulfide-containing resins. *Dent. Mater.* 26, 1010-1016.
- Plimpton, S., 1995. FAST PARALLEL ALGORITHMS FOR SHORT-RANGE MOLECULAR-DYNAMICS. *Journal of Computational Physics* 117, 1-19.
- Rottach, D.R., Curro, J.G., Budzien, J., Grest, G.S., Svaneborg, C., Everaers, R., 2007. Molecular dynamics simulations of polymer networks undergoing sequential cross-linking and scission reactions. *Macromolecules* 40, 131-139.
- Rowan, S.J., Cantrill, S.J., Cousins, G.R.L., Sanders, J.K.M., Stoddart, J.F., 2002. Dynamic covalent chemistry. *Angewandte Chemie-International Edition* 41, 898-952.
- Rubinstein, M., Semenov, A.N., 1998. Thermoreversible gelation in solutions of associating polymers. 2. Linear dynamics. *Macromolecules* 31, 1386-1397.
- Rubinstein, M., Semenov, A.N., 2001. Dynamics of entangled solutions of associating polymers. *Macromolecules* 34, 1058-1068.
- Ryu, J., D'Amato, M., Cui, X., Long, K.N., Qi, H.J., Dunn, M.L., 2012. Photo-origami-Bending and folding polymers with light. *Applied Physics Letters* 100, 161908.
- Scott, T.F., Schneider, A.D., Cook, W.D., Bowman, C.N., 2005. Photoinduced plasticity in cross-linked polymers. *Science* 308, 1615-1617.
- Semenov, A.N., Rubinstein, M., 1998. Thermoreversible gelation in solutions of associative polymers. 1. Statics. *Macromolecules* 31, 1373-1385.

- Shaw, M.T., MacKnight, W.J., 2005. Introduction to Polymer Viscoelasticity, 3rd Edition. Blackwell Science Publ, Oxford.
- Smallenburg, F., Leibler, L., Sciortino, F., 2013. Patchy Particle Model for Vitrimers. *Physical Review Letters* 111.
- Stukalin, E.B., Cai, L.-H., Kumar, N.A., Leibler, L., Rubinstein, M., 2013. Self-Healing of Unentangled Polymer Networks with Reversible Bonds. *Macromolecules* 46, 7525-7541.
- Sun, H., 1995. AB-INITIO CALCULATIONS AND FORCE-FIELD DEVELOPMENT FOR COMPUTER-SIMULATION OF POLYSILANES. *Macromolecules* 28, 701-712.
- Taynton, P., Yu, K., Shoemaker, R.K., Jin, Y.H., Qi, H.J., Zhang, W., 2014. Heat- or Water-Driven Malleability in a Highly Recyclable Covalent Network Polymer. *Advanced Materials* 26, 3938-3942.
- Varshney, V., Patnaik, S.S., Roy, A.K., Farmer, B.L., 2008. A molecular dynamics study of epoxy-based networks: Cross-linking procedure and prediction of molecular and material properties. *Macromolecules* 41, 6837-6842.
- Wojtecki, R.J., Meador, M.A., Rowan, S.J., 2011. Using the dynamic bond to access macroscopically responsive structurally dynamic polymers. *Nature Materials* 10, 14-27.
- Wu, C., Xu, W., 2006. Atomistic molecular modelling of crosslinked epoxy resin. *Polymer* 47, 6004-6009.
- Wu, P., Van Der Giessen, E., 1992. On improved 3-D non-Gaussian network models for rubber elasticity. *Mechanics research communications* 19, 427-433.
- Wu, P., Van der Giessen, E., 1993. On improved network models for rubber elasticity and their applications to orientation hardening in glassy polymers. *Journal of the Mechanics and Physics of Solids* 41, 427-456.
- Yoshioka, S., Aso, Y., Kojima, S., 2003. Prediction of glass transition temperature of freeze-dried formulations by molecular dynamics simulation. *Pharmaceutical Research* 20, 873-878.
- Yu, K., Taynton, P., Zhang, W., Dunn, M.L., Qi, H.J., 2014. Reprocessing and recycling of thermosetting polymers based on bond exchange reactions. *Rsc Advances* 4, 10108-10117.